molecular solid acts as a metallic solid. As shown in Fig. 1, the energy separation is ultimately 1.6 eV. This is remarkably close to that observed in photoemission from negatively charged C_{60} ions in the gas phase (*21*), despite obvious changes induced by K. The apparent position of the LUMO and HOMO bands again appears too far from E_F when the Fermi level energy reference is no longer pinned to an intrinsic level of the molecular system. This accounts for much of the shift observed between the spectra of Fig. 1 for 70- and 100-min exposures. Examination of the distribution of empty states of C_{60} measured with inverse photoemission (bottom curve) shows that the first and second features are separated by $\sim$1 eV. In the ground state, the conduction band of K_6C_{60} probably lies $\sim$1 eV above the valence band. The fact that no emission is observed above the LUMO-derived bands for 100 min and that the LUMO peak lies far below E_F confirms the picture that an insulating molecular solid is formed after full intercalation with all three LUMO-derived bands occupied. Hence, the stoichiometry is K_6C_{60} for that crystal.

Exposure of a K_6C_{60}-based film (characterized by the spectrum for 100-min exposure) to additional K deposition resulted in the nucleation of K metal on the surface. This was reflected by a metallic Fermi level. There were no changes in the valence bands that would indicate that a second unoccupied band was being filled. Annealing of the sample to enhance K intercalation resulted in the elimination of the emission at E_F and a slight sharpening of the valence band features. The inability to force appreciable additional K incorporation is consistent with the filling of all available tetrahedral sites of the bcc lattice (*16*). The addition of more ions of K would start populating the next group of bands of C_{60} which are $\sim$1 eV higher in energy. This would reduce the enthalpy of reaction by the same amount, making it negative so that reaction would be unfavorable.

Finally, the annealed sample was exposed to molecular oxygen in situ. The result was the formation of K-oxide, the leaching of K from the intercalated film, and the loss (to measurements with our surface sensitivity) of emission from the fullerenes. This is consistent with the results of Haddon *et al.* (*13*) that showed severe degradation upon exposure to air.

The results of Fig. 1 explain the changes in conductivity (*13*) and the return to insulating character after complete K incorporation. In the metallic state, they indicate that the conduction band states of K_xC_{60} are C p_π-derived but are disordered. Insight into the mechanism responsible for superconductivity at 18 K can be gained by comparing the results for K_xC_{60} to those for intercalated graphite (*22*). Superconductivity in the 0.15 to 0.55 K range for KC_8, RbC_8, and CsC_8 and its absence in LiC_6 and the higher stage intercalates has been explained by scattering between carbon π states and partially occupied cation *s* states (*22*). Electron-phonon scattering within the graphite layers is believed to be too weak to explain the superconducting properties.

From the McMillan equation, a superconducting transition temperature of 18 K in K_xC_{60} would imply that the electron-phonon coupling constant, λ, would be 0.65 if we assume that the Coulomb pseudopotential is $\mu^* = 0.1$ and the Debye temperature is 700 K. Reasonable assumptions about the range of the Debye temperature and μ^* lead to values of λ between 0.5 and 1.0 such that the system is characterized by strong electron-phonon coupling. For graphite intercalated compounds, the coupling constant is small, $\lambda \sim 0.25$. Since the calculated density of states at the Fermi level is smaller in K_xC_{60} than in intercalated graphite, this implies that the electron-phonon coupling is substantially stronger in the fulleride. In C_{60}, the curvature of the bonding network induces *s-p* hybridization in the π states (which should more accurately be called mostly-π or π-like states). Such hybridization would enhance the single site matrix elements for electron scattering between two mostly-π states by phonons (*4*), and this could explain the stronger coupling and the higher transition temperatures in the fulleride.

REFERENCES

1. H. W. Kroto, J. R. Heath, S. C. O'Brien, R. F. Curl, R. E. Smalley, *Nature* **318**, 162 (1985).
2. R. Taylor, J. P. Hare, A. K. Abdul-Sada, H. Kroto, *J. Chem. Soc. Chem. Commun.* **20**, 1423 (1990); R. Tycko *et al.*, *J. Phys. Chem.* **95**, 518 (1991); C. Yannoni, R. D. Johnson, G. Meijer, D. S. Bethune, J. R. Salem, *ibid.*, p. 9.
3. J. M. Hawkins, A. Meyer, T. A. Lewis, S. Loren, F. J. Hollander, *Science* **252**, 312 (1991).
4. J. L. Martins, N. Troullier, M. C. Schabel, in preparation.
5. For O_2-C_{60} interactions, see G. H. Kroll, P. J. Benning, Y. Chen, T. R. Ohno, J. H. Weaver, *Chem. Phys. Lett.*, in press.
6. S. C. O'Brien, J. R. Heath, R. F. Curl, R. E. Smalley, *J. Chem. Phys.* **88**, 220 (1988).
7. W. Krätschmer, L. D. Lamb, K. Fostiropoulos, D. R. Huffman, *Nature* **347**, 354 (1990).
8. R. M. Fleming *et al.*, *Mat. Res. Soc. Symp. Proc.*, in press.
9. J. H. Weaver *et al.*, *Phys. Rev. Lett.* **66**, 1741 (1991).
10. M. B. Jost *et al.*, *Phys. Rev. B*, in press; M. B. Jost *et al.*, in preparation.
11. J. L. Martins, N. Troullier, J. H. Weaver, *Chem. Phys. Lett.*, in press.
12. S. Saito and A. Oshiyama, *Phys. Rev. Lett.* **66**, 2637 (1991); Q. Zhang, J.-Y. Li, J. Bernhole, *ibid.*, p. 2633; J. W. Mintmire, B. I. Dunlap, D. W. Brenner, R. C. Mowrey, C. T. White, *Phys. Rev. B*, in press.
13. R. C. Haddon *et al.*, *Nature* **350**, 320 (1991).
14. A. F. Hebard *et al.*, *ibid.*, p. 600.
15. H. Herold in *Intercalated Materials*, F. Levy, Ed. (Reidel, Dordrecht, 1979), pp. 323–421.
16. O. Zhou *et al.*, *Nature*, in press.
17. R. E. Haufler *et al.*, *Mat. Res. Soc. Symp. Proc.*, in press; *J. Phys. Chem.* **94**, 8634 (1990).
18. Y. Z. Li, J. C. Patrin, M. Chander, J. H. Weaver, L. P. F. Chibante, R. E. Smalley, *Science* **252**, 547 (1991).
19. R. E. Haufler, L.-S. Wang, L. P. F. Chibante, C. Jin, J. Conceicao, Y. Chai, R. E. Smalley, *Chem. Phys. Lett.*, in press.
20. A Bansil and M. Pessa, *Physica Scripta T* **4**, 52 (1983).
21. S. H. Yang, C. L. Pettiette, J. Conceicao, O. Cheshnovsky, R. E. Smalley, *Chem. Phys. Lett.* **139**, 233 (1987).
22. R. Al-Jishi, *Phys. Rev. B* **28**, 112 (1983).
23. This work was supported by the Office of Naval Research, the National Science Foundation, the Robert A. Welch Foundation, and the Minnesota Supercomputer Institute. The measurements were done at the Wisconsin Synchrotron Radiation Center. Stimulating discussions with Y. Chen, M. B. Jost, G. H. Kroll, T. R. Ohno, D. M. Poirier, and N. Troullier are gratefully acknowledged. We thank R. C. Haddon, J. E. Fischer, and their co-workers for sharing results prior to publication.

19 April 1991; accepted 14 May 1991

Photoemission Spectra and Electronic Properties of K_xC_{60}

G. K. WERTHEIM, J. E. ROWE, D. N. E. BUCHANAN, E. E. CHABAN, A. F. HEBARD, A. R. KORTAN, A. V. MAKHIJA, R. C. HADDON

Photoemission spectra of vacuum deposited layers of C_{60}, before and after exposure to K vapor, show that the K donates its conduction electron into the band derived from the lowest unoccupied molecular orbital. A compound with composition of K_3C_{60}, corresponding to the maximum conductivity, has been prepared. In it the potassium atoms presumably occupy both the octahedral and the two tetrahedral interstitial sites of the face-centered-cubic (fcc) C_{60} structure.

THE DISCOVERY OF NEW METHODS of synthesis of fullerene carbon molecules (*1*) has led to a proliferation of studies of the properties of solid C_{60} (*2–6*). Most of these studies show that the solid form of C_{60} is highly molecular in nature with electronic structure (*2, 3*) that differs little from that of the gas phase molecule.

AT&T Bell Laboratories, Murray Hill, NJ 07974.

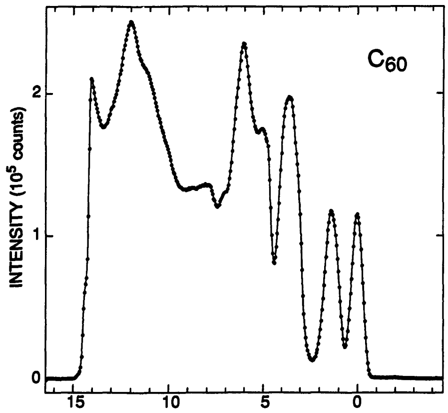

Fig. 1. Valence band photoemission spectrum of a vacuum-deposited C_{60} film, taken with He I resonance radiation. The zero of energy is placed at the HOMO.

However, recent reports demonstrate that the reaction of C_{60} with alkali metal vapor results in a material with metallic conductivity (*4*), which becomes superconducting at low temperature (*5*). These new results have prompted an investigation of the electronic structure of potassium-doped C_{60} using photoemission spectroscopy.

The samples used in this investigation were prepared by vacuum deposition of C_{60} vapor from a collimated pyrolytic BN crucible onto Si(100) substrates within the ultrahigh vacuum (UHV) measurement chamber of the photoelectron spectrometer. The photoemission spectra were obtained with a 50-mm hemispherical electron spectrometer and He resonance radiation, using He I (21.2 eV) for the valence band of the C_{60} and He II (40.8 eV) for the K 3*p* core electrons. The reaction with the K vapor was also carried out in the UHV chamber of the spectrometer, using vapor generated from a commercial SAES Getters source. Superconducting samples have been prepared by the same technique.

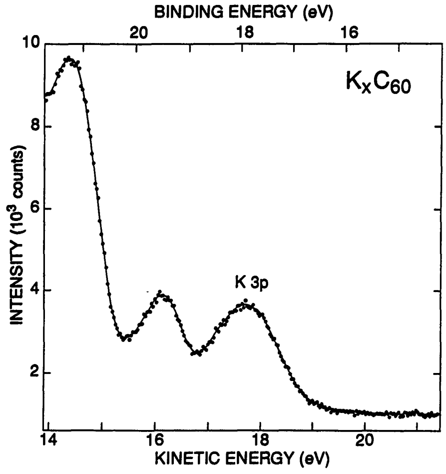

Fig. 2. K 3*p* photoemission spectrum of K_3C_{60} film at room temperature, taken with He II radiation. The peaks at 14.4 and 16.2 eV are due to the excitation of valence band states by residual He I radiation.

A spectrum obtained from a clean, polycrystalline layer is shown in Fig. 1. The highest lying peak to which we have assigned the zero of the binding energy scale is the band derived from the highest occupied molecular orbital (HOMO). The sharp cutoff near 14.4 eV corresponds to the deepest state which can just be excited to the vacuum level. Subtracting the cutoff energy from the photon energy defines the position of the vacuum level. The resulting ionization potential of solid C_{60} is 6.8 eV. This is somewhat smaller than the ionization potential of gas phase molecular C_{60}, which is 7.6 eV (*2*).

When a thin sample is exposed to K vapor at room temperature a strong K 3*p* signal is obtained, but the valence band spectrum becomes weak and featureless. The full width at half maximum of the K 3*p* doublet is much greater than the 0.02 eV of natural width or the 0.26 eV spin-orbit splitting of bulk K metal, suggesting either that many inequivalent sites are occupied or that there is substantial phonon broadening. With the sample in this condition, the valence band spectrum is broadened and attenuated, indicating that there is at least a monolayer of K adsorbed on the surface. (The electron mean free path in metallic K is of the order of the layer spacing at this kinetic energy.) The loss of the resolved structure in the valence band is presumably due to the interaction of the surface C_{60} molecules with the adsorbed K layer.

After heating the sample to ~150° to 175°C, the intensity of the K 3*p* signal decreases, narrows slightly, and shifts to higher binding energy. Presumably some of the potassium diffuses from the surface into the bulk, although a small amount may evaporate. The resulting He II spectrum is shown in Fig. 2 with the K 3*p* peak near 18 eV kinetic energy. (The two lines at lower kinetic energy are due to the excitation of the two most weakly bound features of the valence band, excited by residual He I radiation.) The binding energy of the K 3*p* electrons, with zero assigned to the highest occupied band at 35.7 eV kinetic energy, is 18.0 eV. The remaining K now occupies the interstitial sites in the fcc C_{60} lattice. Since there are only two types of sites available for the K, one octahedral and two tetrahedral per C_{60} molecule, the large width of the K 3*p* signal must be due to phonon broadening. Comparable phonon widths are commonly found for sub-monolayer alkali adsorbates on metals and semiconductors (*7*).

More interesting is the fact that on exposure to small amounts of K a new band starts to appear at the Fermi level (see Fig. 3b). On further exposure it grows into a band located just below the Fermi level (see Fig. 3c). The structure of the rest of the valence band is largely recovered, but the bands are shifted to smaller binding energy and remain wider than in the native film. For this range of composition, essentially identical spectra have also been obtained with Rb. The new band, which lies 1.7 eV above the HOMO of C_{60}, corresponds to emission from electrons donated into the lowest unoccupied molecular orbital (LUMO) by the potassium. The shift is somewhat smaller than the gap between the HOMO and the LUMO in the clean film (1.9 eV) inferred from the C 1*s* energy loss spectrum (*3*). However, this gap may well change with the occupation of the interstitial sites. We can rule out the possibility that we are detecting the signal of the K 4*s* electron, because the photoelectric cross section of that state per electron is almost two orders of magnitude smaller than that of the C 2*p* level for 21.2 eV photons.

From the intensity of the newly occupied level we can determine the composition of the near-surface layer, which is sampled by photoemission. The intensity of the band derived from the LUMO is about one-third that of the HOMO band. Since the latter contains ten electrons (*3, 8*), the composition of the K-doped layer near the surface is K_3C_{60}, provided the photoelectric cross sections are the same for the HOMO and LUMO. Since the 1.38 Å ionic radius of K^+ is only slightly larger than that of the tetrahedral site (1.12 Å) and smaller than that of the octahedral site (2.06 Å), it is tempting to postulate that K_3C_{60} can be described simply by the filling of these sites, resulting in the BiF_3 structure (*9*). With three electrons donated into the LUMO-derived band it is half filled, resulting in maximum conductivity.

The ionization potential of this newly occupied level in the K-doped film is ~4.3 eV. This value is not as well determined as that of the native compound, because the high binding energy cutoff is not as sharp in the doped material. This indicates that the K-intercalated C_{60} compound is not entirely homogeneous and may account for the increased width of the valence band features shown in Fig. 3. This is not unexpected since electrical conductivity measurements indicate that as many as six K atoms per C_{60} molecule can be intercalated (*4*). Indeed, on further exposure to K vapor the spectrum changes significantly. The bands broaden and shift to larger binding energy, and the LUMO peak increases in area and develops a tail toward the Fermi energy. This is presumably an indication of the phase tran-

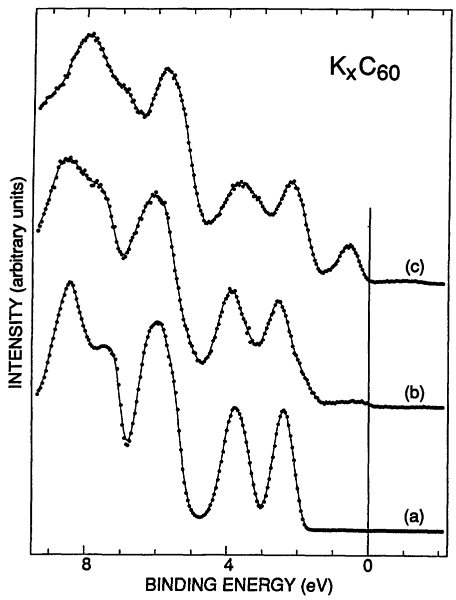

Fig. 3. Valence-band photoemission spectra of K_xC_{60} films prepared by vacuum doping, compared to that of C_{60}. The zero of the energy scale is at the Fermi level of the spectrometer, determined from the Fermi cutoff in In.

sition to the bcc (body-centered-cubic) structure, which can accommodate six interstitials per molecular C_{60} unit.

The apparent similarity between the reaction of C_{60} with K and the formation of graphite intercalation compounds is, at first sight, surprising. Graphite is a semimetal with strongly dispersing π bands that overlap at the Fermi energy. Solid C_{60} is a molecular insulator with narrow bands and a gap of 1.9 eV between the HOMO and LUMO. Nevertheless, there is no doubt that in both materials a metal results from the donation of alkali conduction electrons into unoccupied states of the native material. However, it appears that in solid C_{60} the charge transfer is nearly complete, that is, one electron is transferred per intercalated K atom. In graphite intercalation compounds the charge transfer inferred from measurements of photoemission intensity near the Fermi energy is less than unity, with a value of 0.3 obtained for Cs (*10*). However, band mapping of LiC_6 shows that the Li 2*s* band lies above the Fermi level and that the rigid band model is not obeyed (*11*).

REFERENCES

1. W. Krätschmer, L. D. Lamb, K. Fostiropoulos, D. R. Huffman, *Nature* **347**, 354 (1900).
2. D. L. Lichtenburger, K. W. Nebesny, C. D. Ray, D. R. Huffman, L. D. Lamb, *Chem. Phys. Lett.* **176**, 203 (1991).
3. J. H. Weaver *et al.*, *Phys. Rev. Lett.* **66**, 1741 (1991).
4. R. C. Haddon *et al.*, *Nature* **350**, 320 (1991).
5. A. F. Hebard *et al.*, *ibid.*, p. 600.
6. R. M. Fleming *et al.*, *Mater. Res. Soc. Symp. Proc.* **206**, in press.
7. D. M. Riffe, G. K. Wertheim, P. H. Citrin, *Phys. Rev. Lett.* **64**, 571 (1990).
8. R. C. Haddon, L. E. Brus, K. Raghavachari, *Chem. Phys. Lett.* **125**, 459 (1986).
9. A. F. Wells, *Structural Inorganic Chemistry* (Clarendon Press, Oxford, ed. 5, 1986), p. 422.
10. P. Oelhafen, P. Pfluger, E. Hauser, H.-J. Güntherodt, *Phys. Rev. Lett.* **44**, 197 (1980).
11. W. Eberhardt, I. T. McGovern, E. W. Plummer, J. E. Fischer, *ibid.*, p. 200.

22 April 1991; accepted 15 May 1991

Molecular Beam Scattering from Liquid Surfaces

MARY E. SAECKER, STEVEN T. GOVONI, DANIEL V. KOWALSKI,
MACKENZIE E. KING, GILBERT M. NATHANSON*

By means of controlled collisions of atoms and molecules with liquid surfaces, molecular beam experiments can be used to probe how gases stick to, rebound from, and exchange energy with molecules in the liquid phase. This report describes measurements of energy exchange in collisions between gases (neon, xenon, and sulfur hexafluoride) and polyatomic liquids (squalane and perfluoropolyether). Energy transfer depends critically on liquid composition and is more efficient for the hydrocarbon than for the perfluorinated ether.

COLLISIONS BETWEEN GAS-PHASE and liquid-phase molecules are the first step in establishing mechanical, thermal, and chemical equilibrium between gases and liquids. Gas-phase molecules striking a liquid can scatter immediately away or they can bind to liquid-phase molecules at the surface on their way to solvation, reaction, film formation, or evaporation. These elementary processes can be probed by molecular beam scattering techniques that are widely applied to gas-gas and gas-solid chemical reactions (*1*). By directing beams of atoms and molecules at liquids of low vapor pressure in vacuum, we are learning how gases stick to, rebound from, and exchange energy with organic and inorganic liquids. Scattering experiments on liquids have been performed only rarely (*2*). We describe here studies to measure the exchange of energy when gases (Ne, Xe, and SF_6) collide with polyatomic liquids (perfluoropolyethers and hydrocarbons). Our experiments show that the amount of energy transferred on impact depends critically on the nature of the liquid.

We used two liquids: squalane, a long-chain hydrocarbon, and Krytox 1506, a long-chain perfluorinated polyether (PFPE). Squalane (99.9%, Aldrich), 2,6,10,15,19,23-hexamethyltetracosane, has a density of 0.81 g/cm^3, a vapor pressure below 10^{-7} torr, a surface tension of 30 dyne/cm, and a viscosity of 0.3 poise at 25°C. Krytox 1506 (Du Pont), $F\text{-}[CF(CF_3)CF_2O]_{14(avg)}\text{-}CF_2CF_3$, has a density of 1.88 g/cm^3. Its vapor pressure lies below 4×10^{-7} torr, and it has a surface tension of 18 dyne/cm and a viscosity of 1.3 poise.

The liquids are placed inside a high-vacuum chamber to remove ambient gases and to allow the incident beam of atoms or molecules to collide only with the liquid surface. Impinging beams are created by expanding Ne, Xe, or SF_6 mixed with He or H_2 through a pinhole aperture at 295 K. The nearly monoenergetic beam strikes the liquid surface, and the recoiling species are monitored by a mass spectrometer oriented at 90° to the incident beam. The raw data are time-of-flight (TOF) spectra that record the time for the scattered species to travel 19.5 cm from a slotted wheel to the mass spectrometer. The spinning wheel chops the scattered beam into 11- or 28-μs pulses to measure arrival times. In these studies, the liquid surface is oriented at 45° with respect to both the incident beam and the mass spectrometer; the peak arrival times, however, do not change with surface rotation.

Clean and continuously renewed liquid surfaces are produced by two methods shown in Fig. 1. In one method (Fig. 1A), a vertical, ribbon-like stream is produced by liquid flowing through a highly polished stainless steel jet with a rectangular exit slit 5.0 mm by 0.3 mm (*3*). The incident beam strikes the planar liquid surface (moving at 100 cm/s) as it leaves the jet. The stream is then recirculated by a vacuum-sealed gear pump. A second method (Fig. 1B) uses a slowly rotating wheel that is partially immersed in a liquid reservoir (*4*). The wheel drags along a thin liquid film that is scraped by a razor blade, leaving behind a liquid layer 0.25 mm deep. The molecular beam strikes the freshly wiped surface 0.25 s later. Laser reflections from the fresh surface show that it is macroscopically flat to within 0.5°. The data presented here were recorded with

---

Department of Chemistry, University of Wisconsin-Madison, Madison, WI 53706.

*To whom correspondence should be addressed.